Biophysical Journal
Computational Tool

Biophysical Society

Deep-LASI, single-molecule data analysis software

Pooyeh Asadiatouei,[1] Clemens-Bässem Salem,[1] Simon Wanninger,[1] Evelyn Ploetz,[1,*] and Don C. Lamb[1,*]
[1]Department of Chemistry and Center for NanoScience (CeNS), Ludwig-Maximilians-Universität München, Munich, Germany

ABSTRACT By avoiding ensemble averaging, single-molecule methods provide novel means of extracting mechanistic insights into function of material and molecules at the nanoscale. However, one of the big limitations is the vast amount of data required for analyzing and extracting the desired information, which is time-consuming and user dependent. Here, we introduce Deep-LASI, a software suite for the manual and automatic analysis of single-molecule traces, interactions, and the underlying kinetics. The software can handle data from one-, two- and three-color fluorescence data, and was particularly designed for the analysis of two- and three-color single-molecule fluorescence resonance energy transfer experiments. The functionalities of the software include: the registration of multiple-channels, trace sorting and categorization, determination of the photobleaching steps, calculation of fluorescence resonance energy transfer correction factors, and kinetic analyses based on hidden Markov modeling or deep neural networks. After a kinetic analysis, the ensuing transition density plots are generated, which can be used for further quantification of the kinetic parameters of the system. Each step in the workflow can be performed manually or with the support of machine learning algorithms. Upon reading in the initial data set, it is also possible to perform the remaining analysis steps automatically without additional supervision. Hence, the time dedicated to the analysis of single-molecule experiments can be reduced from days/weeks to minutes. After a thorough description of the functionalities of the software, we also demonstrate the capabilities of the software via the analysis of a previously published dynamic three-color DNA origami structure fluctuating between three states. With the drastic time reduction in data analysis, new types of experiments become realistically possible that complement our currently available palette of methodologies for investigating the nanoworld.

SIGNIFICANCE Single-molecule experiments are very powerful but, at the same time, the analysis can be very time intensive. Here, we present a software that eases the analysis of single-molecule time traces. We have incorporated machine learning methods to support the data analysis. The software performs all steps required for such an analysis either manually or automatically starting from data extraction through to the final graphical outputs. Hence, the time investment needed for the analysis of single-molecule data can be reduced from days or even weeks to minutes.

INTRODUCTION

The ability to detect individual molecules has revolutionized the way we investigate the physical world. When measurements are no longer limited by ensemble averaging, sample heterogeneities, subpopulations and dynamic processes are directly observable. With such high sensitivity, a minimal amount of sample is necessary and, as the analysis is done one molecule at a time, high purification of the sample can be performed in the analysis (1). When performing measurements on immobilized molecules with methods such as atomic force microscopy, optical and magnetic tweezers (2), or total internal reflection fluorescence (TIRF) microscopy, the dynamic processes of a single molecule can be observed as a function of time (3,4). As a result of such measurements, a huge number of trajectories are typically produced that need to be analyzed to extract the desired information from the system of interest.

Among the various valuable single-molecule techniques, Förster resonance energy transfer (FRET) experiments stand out as a noncontact method that can detect distances on the 2–10 nm scale and measure dynamics processes from nanoseconds to kiloseconds. Recent studies have shown that single-molecule FRET (smFRET) experiments are reproducible with an accuracy of 0.6 nm (5,6). With smFRET, it becomes possible to gain insights about the structural features and dynamics of materials, such as the structural fluctuations in biomolecules resulting from complex biological interactions (7). Notably, smFRET promises

Submitted November 30, 2023, and accepted for publication February 19, 2024.

*Correspondence: evelyn.ploetz@lmu.de or d.lamb@lmu.de

Pooyeh Asadiatouei, Clemens-Bässem Salem, and Simon Wanninger contributed equally to this work.

Editor: Robert Best.

https://doi.org/10.1016/j.bpj.2024.02.013

to be an important method for the upcoming age of dynamic structural biology (8). For many experiments, it is possible to detect subpopulations and measure dynamics directly from the collected data. For a detailed quantitative analysis, there are additional steps that need to be performed. Here, it is useful to monitor the fluorescence of the acceptor directly, which can be done using alternating laser excitation (ALEX) (9). In ALEX, the donor and acceptor molecules are excited alternately. Hence, the photophysical state of the acceptor can be probed during the smFRET experiment, and correction factors for the determination of accurate FRET efficiencies can be extracted (10–12). When analyzing ALEX data, the excitation scheme needs to be determined and incorporated into the analysis. As experiments grow in complexity, the intricacy of the analysis increases as well, and the availability of more advanced analysis tools becomes increasingly important.

Numerous software packages have been developed to aid in the analysis of single-molecule measurements. The choice of the optimal analysis tool depends upon the specifics of the experimental system and analysis required for the study. For smFRET experiments, Lerner et al. recently summarized and published an extensive list of analysis tools that were released until the year 2021 including tools to analyze time trajectories from surface experiments (8). In a later study, Götz et al. compared the performance of 11 widely used smFRET analysis tools regarding the determination of kinetic models and extraction of the rate constants (13). With respect to smFRET experiments, the vast majority of software has been developed for two-color FRET experiments (14–19). Our group has also developed a MATLAB-based software for data analysis on two-color FRET systems for surface-immobilized molecules called Tracy (13,20).

Upon expanding our single-molecule TIRF setup to accommodate three-color FRET experiments, we needed to expand our analysis software. With this paper, we introduce our new software, Deep-LASI (deep learning-assisted single-molecule imaging analysis), an open-source software package using MATLAB (but also available as a runtime version) that incorporates Python and C++ routines. The Deep-LASI software offers both manual and automatic analysis environments for a wide range of one-, two- and three-color single-molecule experiments (21). The features of the software include mapping of multiple detection channels, extraction and background correction of one-, two- and three-color FRET data, trace classification and selection of relevant time points for the analyses, determination of the correction factors for the calculation of accurate FRET efficiencies, histogram generation of various parameters, and kinetic analyses using hidden Markov models (HMMs) and deep neural networks. Deep learning techniques are emerging in virtually all data-driven fields and are having a big impact in the life sciences, in particular in microscopy (22–27). Inspired by these developments, we incorporated deep learning to help in trace classification, determination of the relevant regions of relevant traces, automated FRET correction and kinetic analyses.

Deep-LASI supports various data file formats with extendable support to read in new formats into the software. Although originally written for smFRET data, the software is adept at handling any data as long as it results in time traces. Furthermore, the software offers environments for simulating and training single-molecule time traces. We also provide example data sets and tutorials to help users quickly gain proficiency in using the software (28).

RESULTS AND DISCUSSION

Deep-LASI is a user-friendly software package with a high degree of automation and compatibility for the analysis of time-resolved single-molecule intensity traces. It is designed to help with the data analysis of one-, two- and three-color FRET experiments with interactive graphical user interfaces (GUIs) to provide enough freedom so that the user can extract the desired information based on their analysis needs. The source code is available such that the software can be adapted and further developed by expert users and software developers (29). A description of the implemented features is given in the following sections.

The information to be extracted from the intensity traces of single molecules and the necessary steps will vary depending on the measurement assay and question of interest. An overview of the most common procedures in single-molecule data analysis is summarized in Fig. 1. The main analysis steps include reading in the raw data, mapping the detection channels, (co-)localizing the particles and extracting the intensity information over the measurement time. In the next step, the software allows for classifying traces, determining usable regions within each time trace, plotting the distributions of the extracted parameters (such as FRET values, labeling stoichiometry or dwell times), calculating the necessary correction factors and performing a kinetic analysis in the case of a dynamic system. In the case of the kinetics analyses, transition density plots (TDPs) are automatically generated and provide access to the cumulative dwell-time distribution functions (CDFs).

Deep-LASI also offers the opportunity for expert users to simulate multicolor smFRET traces and to train neural networks for new single-molecule assays. To ensure flexibility and accessibility overall, the extracted and analyzed data can be saved and reloaded at any time, and can be additionally imported and exported, from and into standard data files. In the following section, we discuss the individual working steps and underlying mechanisms that define the software's functionality.

Main functionalities of Deep-LASI

Typically, the initial step in analyzing single-molecule experiments involves reading in the raw data. The most

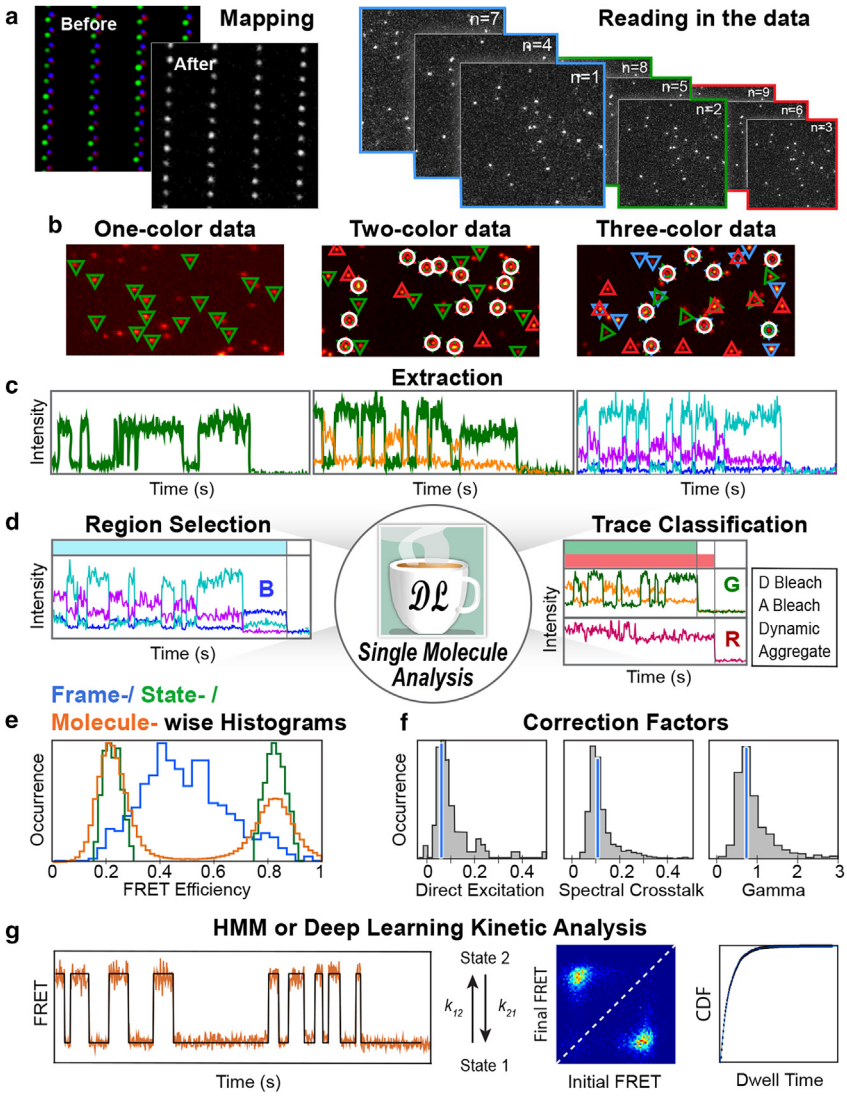

FIGURE 1 Overview of the functionalities of the Deep-LASI software package. The main applications of the software package are to extract, sort and analyze intensity traces from single-molecule data. This process involves a series of key steps: (*a*) for multicolor experiments, the different channels need to be registered to each other (i.e. mapped). Afterward, the raw data is read in for each channel from a stack of frames based on the excitation scheme. (*b*) Single molecules are localized and, when desired, colocalized across different channels based on the created map. (*c*) The intensity traces are extracted from each detected (and colocalized) particle and corrected for background. (*d*) The analysis of extracted intensity traces starts with trace classification and selection of the useful region of each channel where the corresponding fluorophores are active. (*e*) The results can then be visualized by the means of various histograms with frame-, state- and molecule-wise approaches. (*f*) Optionally, the method-specific correction factors are determined. (*g*) For dynamic traces, a kinetic analysis can be performed by hidden Markov modeling (HMM) or deep learning approaches. The panels show a typical state transition path inferred by HMM (i.e. Viterbi path) and transition density plots with state transition information and the cumulative dwell-time distribution function (CDF) determined by fitting, respectively. To see this figure in color, go online.

elaborate features of the software are designed to work with images or movies from cameras like EMCCD (electron-multiplying charge-coupled device) or sCMOS (scientific complementary metal oxide semiconductor) cameras. However, it also accommodates the direct read in of custom, nonimage data file formats encoding a time series (Fig. 2, *blue boxes*). For detailed information and the latest list of supported file formats, please refer to the online tutorial available for Deep-LASI on Read the Docs (28).

Given the diversity of fluorescence-based assays and methods resulting in time traces suitable for analysis through Deep-LASI, we focus on the main functionalities of the software. This includes importing data files, detecting and mapping molecules, extracting traces, calculating background, and manually or automatically sorting the collected data (Fig. 2, *green boxes*). Following these steps, the software provides a set of different tools to spectrally correct, kinetically analyze and summarize the single-molecule data (Fig. 2; *pink boxes*). These tools can be used for 1) determining correction factors, 2) plotting representative properties of the results via their distributions (e.g. of apparent or accurate FRET values of single molecules, of states or frames), 3) allowing unsupervised, kinetic analysis of selected regions of the appropriate traces using HMM or deep learning algorithms and finally, 4) visualizing the data using TDPs and CDF plots. For an in-depth understanding of each feature, including the algorithms involved, the philosophy behind the GUIs, and tutorials featuring specific analysis examples, please refer to the comprehensive software documentation and manual (28).

Channel mapping

For multicolor experiments using separate detection channels, a registration of the different detection channels is

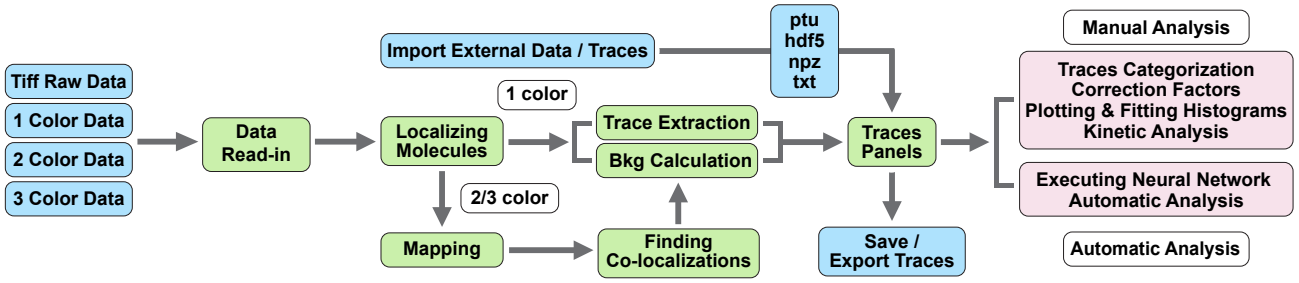

FIGURE 2 Schematic representation of the data-handling workflow using the Deep-LASI software. The blue boxes show the raw movie data and intensity trace files that can be loaded into the software as well as the saving routines for storage and export of the analyzed data. The green boxes show the initial steps for data extraction and preparation with the Deep-LASI software. The pink boxes summarize the tools for data analysis and representation of results available through both manual and automatic modalities. To see this figure in color, go online.

needed. When measuring at different wavelengths, perfect alignment between channels in terms of shift, magnification, and rotation can be challenging and time-consuming. Hence, a mapping process between cameras or regions of interest is required to ensure that the fluorescence signatures visible in the different channels originate from the same immobilized molecule. When performing fluorescence-based single-molecule experiments using imaging, the optimal pixel size is usually in the range of 40–100 nm. Thus, the fluorescence emitted by a single molecule spans multiple pixels, and alignment within a single pixel is sufficient. The mapping is performed using a set of emitters well distributed across the detectors' field of view. We commonly employ a zero-mode waveguide pattern or a surface covered with emitting or scattering particles, such as fluorescent beads. Alternatively, mapping can be accomplished using the actual single-molecule data. One channel is selected as a reference channel. Our software then utilizes a phase-correlation algorithm to estimate the geometric transformation necessary to align the other channels to the reference image (Fig. 3 *a*)(30). This geometric transformation involves scaling, rotation, and translation of the read-in images. Individual emitters are detected based on a user-selected threshold and their localizations are utilized to further refine the mapping using a 2D polynomial of order up to 3. The prerequisite for this refinement operation is the colocalization of individual particles within 2 pixels after application of the geometric transformation. Their positions are determined using a stationary wavelet algorithm with adjustable sensitivity (31). A transformation matrix is generated, which is then used to map the respective coordinates between channels. The mapping step corrects small misalignments between the cameras originating from tilts and shifts of cameras and different magnifications, as well as aberrations in the detection paths. Notably, the mapping function is only used to find the corresponding pixels in the various detection channels corresponding to the location in the reference channel. The actual single-molecule analysis is performed separately on the raw data. No mapping of the images via the transformation matrix is performed except for inspection of the quality of the transformation matrix.

Loading imaging data collected using various excitation schemes

Once the detection channels have been mapped onto each other, the actual single-molecule data one wishes to analyze is loaded. Upon loading the data, the frames are segregated based on the excitation scheme used (when necessary). For accurate smFRET experiments using camera-based data acquisition, it is advantageous to use millisecond ALEX schemes (5,32). For two-color experiments, alternating frames are collected using donor and accepter excitation respectively. Acceptor excitation is used to probe the presence and photoactive state of the acceptor molecule enabling the calculation of labeling stoichiometry. However, frames with acceptor excitation have to be excluded when calculating the FRET efficiency. When expanding to three-color experiments, ALEX is essential for analyzing the data and three excitation lasers are alternated, respectively. There are also experiments where one wishes to detect the presence of one color at the beginning of the experiment, but then perform a smFRET experiment with different colors. One example would be measuring the conformation of DNA using smFRET in the absence or binding of a DNA-binding protein, which is labeled with a third color. In this case, the first few frames are used to detect the presence of the third color at the beginning of the measurement and used for selecting the traces that are to be analyzed. The remainder of the frames from the selected traces are then used to extract the smFRET information.

Typically, a series of consecutive measurements is performed using the same measurement parameters (excitation scheme, detection channels, exposure time, etc.) to gather sufficient statistics. This results in a collection of data files originating from each camera. To initiate the analysis of the entire experiment, the Deep-LASI read-in process begins by collectively selecting all files from a single camera at once, usually starting with the most blue-shifted detection channel. Next, the first movie of the chosen file set is loaded. Here, the user is prompted to define the frame range,

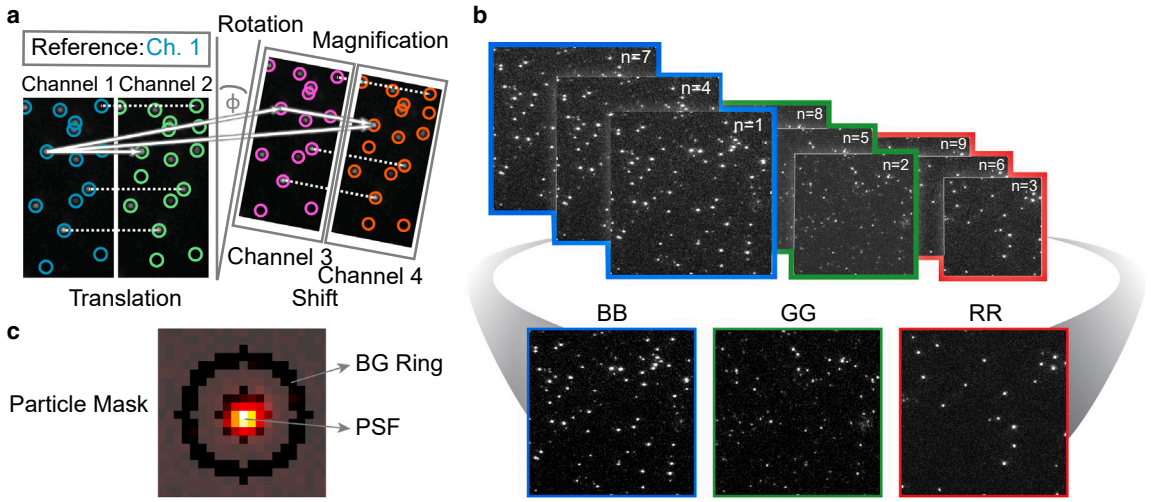

FIGURE 3 Particle detection, localization and mapping. (*a*) Mapping process with Deep-LASI for multicolor experiments: a reference channel is chosen and all other channels are registered with respect to the reference channel. Here, the chosen reference channel is the blue channel. (*b*) For trace extraction, Deep-LASI first opens the images registered on a specific camera and segregates the detection channels according to the excitation scheme. Here, we show the BB, GG, and RR channels. To identify the position of single emitters, we use the cumulative image taken from the direct excitation frames for the respective channels. (*c*) To calculate the measured intensity coming from a detected particle, a mask function is selected. We typically use a particle detection mask having a circular geometry of 7 pixels in diameter. The outer dark ring with a width of 2 pixels is used to determine the background contribution. To see this figure in color, go online.

excitation sequence, and detection channel. Next, a cumulative intensity is displayed over the user-selected range (Fig. 3 *b*) to improve the signal-to-noise ratio and facilitate a user-friendly, interactive parameterization for the trace extraction. The loading procedure is then repeated for the corresponding movies of the remaining channels. The particle detection method and threshold for each detection channel are then determined. In the last step, the extraction parameters are provided by the user: particle and background mask (Fig. 3 *c*), molecule selection criteria and the frame range used for extraction. Once the detection and extraction thresholds are established for all channels, the corresponding sets of files are sequentially loaded and single-molecule traces are extracted according to the given selection mode: Deep-LASI extracts the trajectories 1) for all detected molecules, 2) for colocalized molecules only, or 3) for molecules detected in a given detection channel.

Particle detection

To extract single-molecule trajectories, Deep-LASI provides three different techniques for single-molecule localization. For each technique, a sensitivity threshold is applied based on the normalized reconstruction from weighted wavelet coefficients or intensity values. Based on the selected threshold, a binary image is generated that encodes the detected particles. The position of each particle is determined by the center-of-mass of the pixels associated with the particle.

Wavelet. Wavelets are filters that can be applied to images (or time series) to enhance features with particular spatial (or temporal) frequencies. As the fluorescence signal coming from single molecules are diffraction limited, the detected fluorescence should be symmetric with the size given by the point-spread function. By applying different wavelet filters, the original image is decomposed into a finite number of wavelets where particular spatial features are enhanced and others suppressed. More specifically, by mathematically applying low-pass and high-pass filters on the signal and repeating the procedure, a set of wavelet planes are generated at different resolutions (33–35). Based on the median absolute deviation of the wavelet coefficients for each plane, insignificant features are removed automatically.

Intensity thresholding. Another approach is to use intensity thresholding to detect molecules emitting intensities higher than a user-defined level. When enough adjacent pixels are above the threshold, the area would be considered a particle and the central point taken for trace extraction. This rather easy method works well as long as the signal and background are homogenous over the field-of -view and the signal from the molecules is sufficiently stronger than the background.

Regional maxima. An alternative method based on intensity thresholding is the regional maxima approach. With this method, a Gaussian filter of 9 pixels is first convoluted with the image and then the MATLAB function *imregionalmax* is used to find the local maxima. This is done by locating pixels where all eight neighboring pixels are lower in intensity. The routine then returns all the regional pixels which are a local maximum and are considered as the center of single emitting particles. Pixel intensities below the user-defined threshold are set to zero. These selection criteria have an advantage over normal intensity thresholding when

analyzing data with heterogeneous particle intensities and noise within a frame.

Trace extraction

From the binary image generated from the detected particles, the particle positions are extracted using the MATLAB in-built function *regionprops*. This calculates the centers-of-mass for connected pixels. Using the central position of the individual particles, the particle mask (Fig. 3 *c*) is then used to determine the total number of detected photons for the particle as well as the background contribution. Typically, we use a circular particle mask with a diameter of 7 pixels. The size is chosen to optimize collection of photons within the point-spread function of the molecule while minimizing the inclusion of additional pixels and hence potential overlaps between neighboring particles. The user can also adjust the particle mask settings based on their specific needs.

The particle positions are then linked in consecutive frames to generate time trajectories. To extract the intensity traces from each detected single emitter, frame-wise intensities for each channel are determined, and plotted over the whole measurement or selected frame range.

Background determination

The size and shape of the particle mask surrounding each particle's point-spread function (Fig. 3 *c*) and the method of background determination have a considerable impact on the signal-to-noise ratio, the quality of traces and finally on the resulting histograms. There are multiple approaches to background correction. Fortunately, the number of pixels that can be used to calculate the background intensity far outnumber the number of pixels within the point-spread function and hence can be subtracted with high accuracy. Deep-LASI extracts frame-wise intensities for each molecule detected in the various channel(s). To avoid any potential heterogeneity from the illumination profile, a nonconstant background level within a frame or differences between cameras, the background signal is calculated and subtracted from the accumulated intensity within each particle mask. At any time during the analysis, the user can view the raw intensity traces without background subtraction.

As the signal is averaged in the background mask, no molecules should be present in the region used for determining the background. For densely populated surfaces, the default mask can be adjusted, e.g., by reducing the radius of the mask. To decrease the uncertainty in the background estimation, the background is measured in approximately twice as many pixels as the signal. In addition, as the background does not typically change strongly with time, an 11-frame sliding window (± 5 frames) is used to average the background value. The average background signal (scaled to the number of pixels in the particle mask) is then subtracted from the total measured intensity. The total measured intensity and the local background are determined for each frame and the background-corrected intensity traces stored. By visually checking the intensity level of a trace after photobleaching of all fluorophores, the quality of the background subtraction routine can be controlled. At this point, all the extracted traces from the experiment are saved into a single datafile with a filename adapted from the name of the first movie file with the extension of .tdat.

Trace read-in options

At this point in the analysis, one has extracted and saved the single-molecule time traces from one or more channels for a given excitation scheme. Here, it is also possible to reload the traces as well as to directly import intensity traces extracted using other software for any type of single-molecule time-series data. Several data importing options are incorporated including ptu, hdf5, npz, and txt files. For example, we have also used Deep-LASI to analyze single-molecule intensity traces collected one at a time on a confocal microscope (21). The txt file format is provided (13,28) such that users can convert their data into a format that can be read into Deep-LASI.

Analysis options

Deep-LASI offers diverse tools for analyzing and presenting information derived from single-molecule time traces, irrespective of the methods employed for data acquisition, ranging from one- to three-color measurements: the software facilitates both manual and automatic processes for 1) trace categorization into, for example, usable static and dynamic traces and 2) selection of specific regions within individual traces for further analysis. In addition, 3) Deep-LASI provides an overview of parameters characterizing selected regions in the intensity traces including brightness, background intensity, signal-to-noise ratio. and photobleaching time. Beyond these basic functionalities, Deep-LASI supports manual and automatic analyses of one-, two- and three-color FRET assays. Moreover, the software enables 4) extraction of kinetic information from dynamic traces. Two distinct approaches are available for kinetics analyses: the first involves conventional HMM with selectable algorithms for up to three channels, as detailed below (36,37). The second approach employs neural networks for automated data analysis wherein Deep-LASI outputs a confidence level of the time trajectory being in a specific state for each frame. In addition to kinetic analyses, Deep-LASI allows for 5) the calculation of accurate FRET efficiencies by extracting the necessary FRET correction factors from the data. Finally, the software provides 6) state-of-the-art tools for summarizing the FRET states and kinetics extracted during the analysis. These include histograms illustrating distributions of, e.g., FRET efficiencies (apparent and accurate FRET) of static and dynamic traces, stoichiometry, or FRET correction factors. Furthermore, Deep-LASI provides TDPs and CDFs for summarizing the kinetics information found in the single-molecule data.

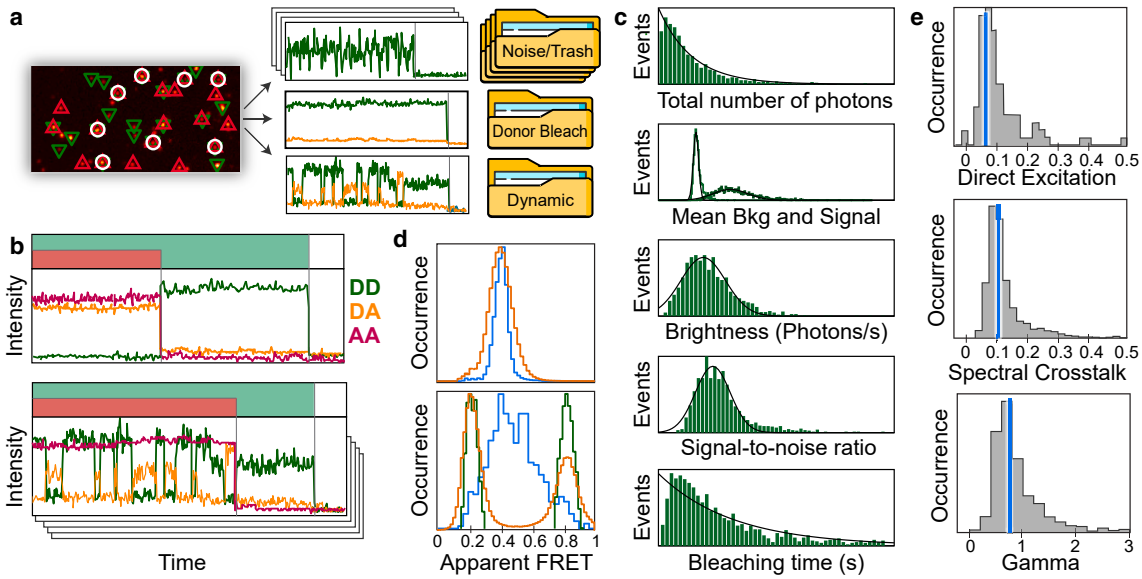

FIGURE 4 Single-molecule trace analysis of 2c FRET data with the Deep-LASI software. (*a*) The analysis of extracted traces begins with categorization based on the 1) underlying single-molecule assay, 2) numbers of dyes, 3) trace quality, 4) photochemistry involved, and 5) dynamic information available. (*b*) Two exemplary intensity traces are shown for two-color smFRET measurements using the ALEX scheme. (*Top*) A molecule exhibiting static FRET and (*bottom*) a dynamic molecule. In both cases, the acceptor molecule photobleaches first leaving fluorescence only from the donor molecule until it photobleaches at the end of the traces. The donor signal (*green*), sensitized acceptor emission (*orange*), and direct acceptor excitation (*red*) are shown. Shadowed regions in green and red mark the selected regions in each detection channel to be considered in further analyses. (*c*) Deep-LASI offers an overview of information from selected regions of the single-molecule traces. In addition to FRET, it displays molecule-wise histograms of signal (Sig) and background intensities (Bkg), brightness (Hz), signal-to-noise ratio, and photobleaching time (s) with the corresponding fits. The histograms shown are for green detection after green excitation. (*d*) SmFRET histograms of (*top*) a static sample and (*bottom*) a dynamic sample interconverting between two states characterized by low and high FRET efficiencies. The apparent FRET efficiency of the sample is depicted frame-wise (*orange*), molecule-wise (*blue*), and state-wise (*bottom panel*, *dark green*). (*e*) Distributions of the FRET correction factors are shown, which are used to correct for direct excitation, spectral crosstalk, and differences in detection sensitivity (gamma) for a simulated two-color smFRET sample. The median values of each histogram are indicated as a blue line. To see this figure in color, go online.

The subsequent sections provide a brief introduction to manually using Deep-LASI for categorizing single-molecule traces, selecting regions, and analyzing static experimental parameters. Subsequently, we discuss how to obtain accurate FRET measurements and extract kinetic information from single-molecule data.

Trace categorization and static analysis

After extracting or loading single-molecule traces, the next step involves the categorization and sorting of the molecules. In a typical single-molecule experiment, the data set can easily comprise several thousands of traces. Many of the traces may be noninformative due to rapid photobleaching, the presence of aggregates, incomplete labeling, or inadequate signal to noise ratios. Hence, the primary objective in trace categorization is to select the suitable regions of appropriate traces for further analysis. This starts by separating out traces that are unsuitable. For this, Deep-LASI provides dedicated panels and GUIs for systematically reviewing and categorizing traces (see Fig. 4 *a*). Typical categories include "static", "dynamic" and "trash" although users have the flexibility to add custom categories as needed for their experiment. Furthermore, Deep-LASI facilitates the sorting of traces based on the number of photoactive fluorophores by considering which fluorophores are active in each frame. For two-color FRET assays, for instance, traces can be sorted into categories like "donor bleach" and "acceptor bleach" which proves instrumental in determining FRET correction factors at a later stage. Notably, users have the flexibility to assign multiple categories to individual traces, allowing classifications such as "static" and "acceptor bleach" simultaneously. This functionality becomes particularly advantageous in three-color FRET experiments where additional statistics for FRET correction factors can be obtained from analyzing constructs that contain only two of the three fluorescent dyes.

In the second step of the characterization procedure, it is necessary to mark the regions of the useful traces to be included in further analyses (Fig. 4 *b*). Selection of the desired regions is possible with an activated cursor on the intensity trace panels. The selection can be general to define the regions in all channels to be included in the final histograms or kinetic analyses, or can be specific to each detection channel (shaded in the corresponding color) for determining individual photobleaching steps and regions to be used for the calculation of FRET correction parameters later on. Once correction factors have been estimated, users can choose to visualize the data at the level of apparent or

accurate FRET. Correction factors are used to account for donor leakage into the acceptor channel, direct excitation of the acceptor, and differences in detection sensitivity of the donor and acceptor molecules. In addition, the individual intensity traces can be displayed with or without background correction.

Statistical overview of selected traces

The Deep-LASI software offers the possibility to evaluate and visualize the characteristics of selected frames, traces and, ultimately, the analytical results. From the first interface, the fluorescence properties of the different fluorophores can be assessed (Fig. 4 *c*). For EMCCD cameras, the characteristics of the amplification can be included to convert the camera counts into approximate photon numbers (otherwise, the signal in camera counts will be plotted). These distributions showcase the total signal until photobleaching (number of photons), the total signal and mean background per molecule (in kHz), the background-corrected brightness for the corresponding channels (in Hz), the individual signal to noise ratios, and the time until photobleaching of the respective fluorophores (in s). The histograms for each channel are automatically fitted to mono-exponential or Gaussian functions. The fit results are given in the respective panels.

smFRET analysis

In our research group, we specialize in smFRET experiments and evaluation. Hence, parts of the software are optimized for smFRET analysis from experiments carried out on immobilized molecules. With FRET, it is possible to investigate structural properties or dynamics due to FRET's strong dependency on the distance between fluorophores (8). From the selected regions of the corresponding molecules, it is possible to calculate the apparent FRET efficiency histograms, that is the FRET efficiency determined from background-corrected intensities without any further corrections. These can be plotted for each frame and molecule (frame-wise) or averaged value determined individually for each molecule (molecule-wise) (Fig. 4 *d*). Frame-wise FRET histograms contain all FRET values obtained across different molecules and frames, giving a comprehensive projection of accessible FRET states in the sample from all selected molecules (Fig. 4 *d*, *orange line*). Alternatively, the molecule-wise (or trace-wise) histogram reports an average FRET value for each single molecule over the selected frame range (Fig. 4 *d*, *blue line*). Notably, for static samples, molecule-wise and frame-wise histograms will coincide whereas, for dynamic molecules, they will not. To overcome this, it is possible to plot histograms state-wise when analyzing dynamic traces (see dynamic analysis below; Fig. 4 *d*, *lower panel*, *green line*).

To capitalize on the ability of FRET to measure distances accurately on the subnanometer regime, it is necessary to correct the apparent FRET efficiency for direct excitation of the acceptor, spectral crosstalk of the donor fluorophore into the acceptor channel and variations in detection sensitivity to the various fluorophores. Depending on which molecule photobleaches first, it is possible to determine a subset of the correction factors directly from the individual traces. In the case where the donor undergoes photobleaching before the acceptor, the software calculates the direct excitation correction factor using the residual emission of the acceptor directly excited by the donor laser excitation (Fig. 4 *e*, *top panel*). Conversely, if the acceptor photobleaches before the donor molecule, the spectral crosstalk correction factor is determined as the residual donor emission detected in the acceptor channel (Fig. 4 *e*, *middle panel*). After correcting the trace for direct excitation and spectral crosstalk, the same trace can be used for determination of the detection efficiency correction factor from the ratio of the changes in acceptor and donor intensity after the acceptor's photobleaching step (Fig. 4 *e*, *bottom panel*). Once all individual traces are assessed for possible contributions to the correction factors, the distribution is plotted and the software computes the average, median, and mode of the distribution for each correction factor and dye pair. For an accurate estimate of the various correction factors, a minimum number of continuous frames after the photobleaching step should be included (we use a minimum of 20 frames). To kick out spurious values from the distributions, a maximum tolerable value for all correction factors can be entered. Values above the maximum will not be included in the calculation of the average, median and mean. The correction factors that cannot be determined directly from the traces are taken from the distribution (referred to as global correction factors). We typically use the median of the distribution as it was found to be most robust given typical statistics, but the average or mode can also be selected (Fig. 4 *e*). The user also has the option to use the global correction factors for all traces or to enter the values individually for each trace. Once the correction factors are determined, accurate FRET values as well as distances can also be displayed. These together with additional parameters such as stoichiometry and FRET efficiencies (both accurate and apparent FRET) can be viewed in a second interface. All histograms can be normalized and/or fit to a wide variety of functions.

Machine learning analysis of dynamic trajectories

To analyze dynamic samples, additional functionalities are available in the Deep-LASI software. One can choose from two HMM analyses (Murphy (37) or Schreiber (36)) or automatically via deep neural networks (DNNs) (21) (Fig. 5 *a*). The results provide an estimation of the underlying states and kinetics within the individual trajectories. Hence, in the end, one generates a "digitalized" version of the state pathway, which allows determination of the transition rates via the CDFs.

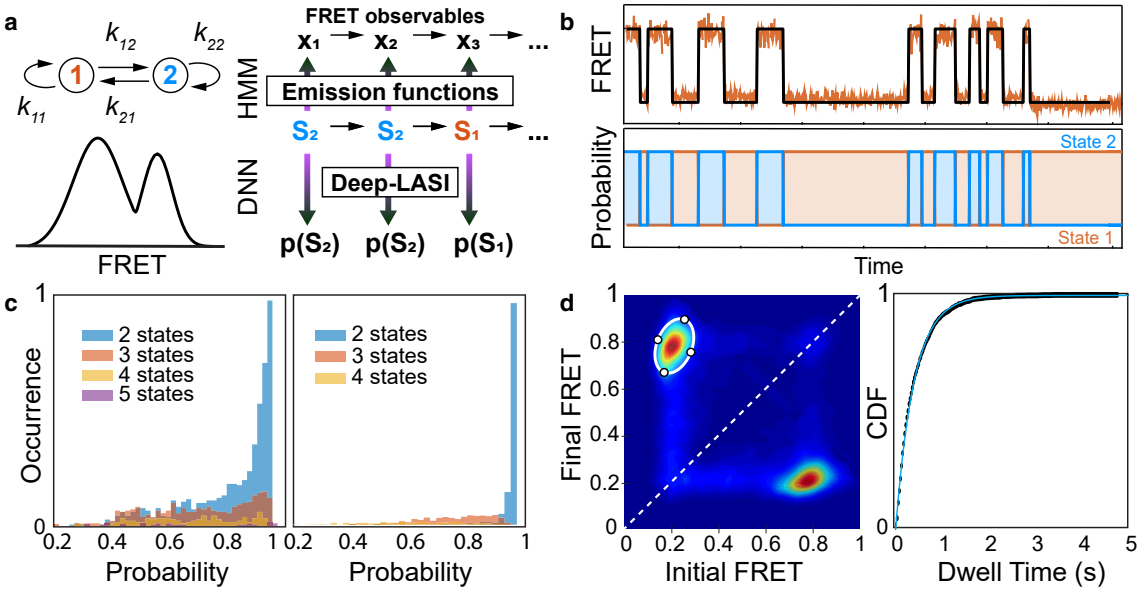

FIGURE 5 Kinetic analysis with the Deep-LASI software. (*a*) Left: schematic representation of a two-state dynamic FRET system with the transition rates (k_{ij}) between the two states. Right: the software extracts the dynamic interconversion rates between the states through an HMM analysis or via state probabilities derived using a deep learning algorithm based either on the measured FRET values or on the intensities directly. (*b*) Results of a kinetic analysis for an exemplary two-state smFRET trace. Top: the FRET trace plotted along with the most probable state path (*black*) generated through an HMM analysis (i.e., the Viterbi path) or via the neural network and (*bottom*) the corresponding state probabilities. (*c*) For an automated kinetic analysis, the neural network identifies the most likely number of detected states in each individual trace (*left panel*). The state path is then determined based on the number of detected states and a histogram of the average confidence of the assigned states in each trace is given (*right panel*). (*d*) Left: to extract the underlying dwell times and kinetic rates, TDPs are generated. By selecting individual clusters in the TDP, which summarize transitions of dynamic molecules from an initial to a final FRET state, the dwell-time distribution for the cluster is calculated. Right: the corresponding CDF for the selected population shown on the left. To see this figure in color, go online.

HMM can be performed on one-, two- and three-color data. For each data type, the FRET efficiencies or the intensities can be used as input. The number of states, mean values, standard deviations and the transition matrix can be initialized either using prior knowledge of the user, random uniform distributions or estimations based on k-means clustering. Other adjustable model parameters include the convergence threshold, the maximum number of iterations, and the choice between local or global HMM. Local HMM creates a new model for each trace, whereas a global HMM utilizes one model (rates and states) for all traces of a selected category. Like other analysis tabs, this analysis can also be exploited on any desired category(s). The states and kinetics of one- and two-color data are straightforward to model as they inherently represent distances in only one dimension. In three-color FRET experiments, distances can be extracted in three dimensions by combining the FRET efficiencies of all fluorophore pairs. However, three-color FRET is complicated by the strong interdependence of the FRET efficiencies and the numerous correction terms that are necessary to convert the apparent FRET efficiencies to actual distances. These corrections introduce significant uncertainties, making it difficult to properly model the system using HMM and identifying state transition. Therefore, the software focuses on using apparent FRET efficiencies and uncorrected intensities to accurately analyze three-color FRET kinetics, treating the states of a given molecule as unique combinations of FRET efficiencies or intensities (38). This is achieved by employing multivariate HMM, where each trace is 2D and each observation is a multivariate vector. In the case of three-color FRET, the multivariate vectors can contain either the three FRET efficiencies or the five intensity channels that are relevant for determining the kinetic information. Direct excitation of the last acceptor is excluded as it provides no kinetic information. Regardless of the number of colors, the software provides the option to use HMM on traces that were manually selected or classified by a DNN.

After running the HMM, multiple corresponding panels with the number of states, state values and transition probability matrices are updated. These will depend upon the executed mode, i.e., local or global. Fig. 5 *a* shows an example of a dynamic, two-state system with independent transitions between these states. On the trace panel of the HMM tab, the individual traces and their corresponding Viterbi path are shown (Fig. 5 *b*, *top panel*). One can click through all traces present in the selected category to check the accuracy of the predicted states and transitions sequences.

DNNs can also be used for the kinetic analysis after the state classification step has been performed (e.g., Fig. 5 *b*, *bottom panel*). Here, there is the option to run a "number

of states" classifier to determine the predicted number of states observed in each trace (Fig. 5 *c*, *left panel*). The user can then run a particular state-classifier model (i.e., for two states, three states, or four states) on the selected data or use the output of the number of states classifier to automatically use the corresponding state-classifier model for state assignment on a trace-by-trace basis. The software plots the average confidence level for the state assignment over the individual traces (Fig. 5 *c*, *right panel*). For the example shown here, the software is very confident regarding the existence of two states and their corresponding state assignments.

After running the machine learning approach of choice (i.e., HMM or DNN), a digitalized state pathway is generated for each trace. This allows one to calculate a state-wise distribution from the state trajectories (Fig. 4 *d*, *bottom panel*, *green line*). The state-wise trajectories can be plotted normalized to the number of transitions or weighted by the number of frames contributing to each state. To analyze the underlying dynamics, the Deep-LASI software utilizes TDPs to visualize the detected transitions between initial and final states within the data (Fig. 5 *d*, *left panel*). From the TDP, the number of states, their corresponding values (e.g. FRET efficiencies), their connectivity and the number of transitions between different pairs of states can be revealed. Transition rates can be obtained directly from the output of a global HMM analysis. Alternatively, they can be calculated by selecting individual populations in the TDP and then fitting the corresponding dwell-time distribution (Fig. 5 *d*, *right panel*).

Automatic analysis

The analysis of single-molecule data, especially for molecules immobilized on a surface, usually takes days or weeks, even for a single day of measurement, and is prone to bias from the person analyzing the data. In addition, due to the time necessary for obtaining a reasonable amount of statistics, the parameter space that can be analyzed via such experiments is limited. To overcome such issues, automatic analysis tools using trained DNNs are available in the Deep-LASI software. Hence, each step of the analysis workflow described for manual evaluation above can be performed automatically. DNNs are available for trace classification (with region selection), number of state determination, and state trajectory analyses, and can be applied individually. In addition, the entire workflow from sorting and categorizing time traces, determining the photobleaching steps, calculating method-specific correction factors and state pathway determination can also be done automatically with the click of a single button (21). After running the automated analysis, the workflow continues with evaluation of the TDPs by selecting clusters and fitting their dwell-time distributions. On typical smFRET measurements with 4000 frames, the automated analysis is performed within 20–100 ms per intensity trace and has been implemented for one-, two- and three-color data.

Currently, we have tested the Deep-LASI software on DNA origami structures as well as protein systems (21). However, the number of possible sorting categories and traces characteristics that the DNN has been trained on is not exhaustive. Therefore, for advanced users, the Deep-LASI software has the option to simulate one-color single-molecule data as well as two- and three-color smFRET traces. In addition, the simulated data can also be used to train new neural networks, if desired.

Additional attributes of Deep-LASI

The motivation for designing and publishing Deep-LASI was manifold. We wanted to develop a software package for the community that 1) is easy to use for everyone independent of their scientific maturity or disciplinary background, 2) contains a high degree of automatization with respect to data extraction and analysis to save time and remove user bias, 3) is compatible with other single-molecule methods and setups with temporal resolution and 4) provides state-of-the-art tools for analyzing single-molecule trajectories. In addition, the software should provide 5) advanced tools for analyzing experimental data from multicolor FRET experiment up to three colors (and potentially up to four in the future). These include the ability to simulate single-molecule data and train new machine learning approaches (HMM and neural networks) that are extendable for future single-molecule assays. Here, we summarize these general aspects of the developed software suite Deep-LASI.

Ease-of use/user friendliness

To make the software easily accessible to a broad range of users and establish a universal analysis environment, Deep-LASI was designed to be easy to learn with a clear workflow. Each step in the workflow is accompanied with its own GUI guiding from reading-in the raw data over data extraction and analysis to visualization of the results. After each step of data processing and analysis, it is possible to save the current status of the project, giving the user complete freedom to stop the analysis and resume at a later point in time. The resulting parameters and plots can be exported to external tools for presentation or publication purposes.

Automation

Gathering sufficient statistics in single-molecule experiments requires collecting data from thousands of single molecules. Hence, the Deep-LASI software can read-in hundreds of consecutive movies and extract the single-molecule traces automatically after the conditions have been determined for the first movie. As data extraction and evaluation can be performed without supervision, new analyses and experiments are now realizable. For example, it is now possible to utilize more of the collected information such

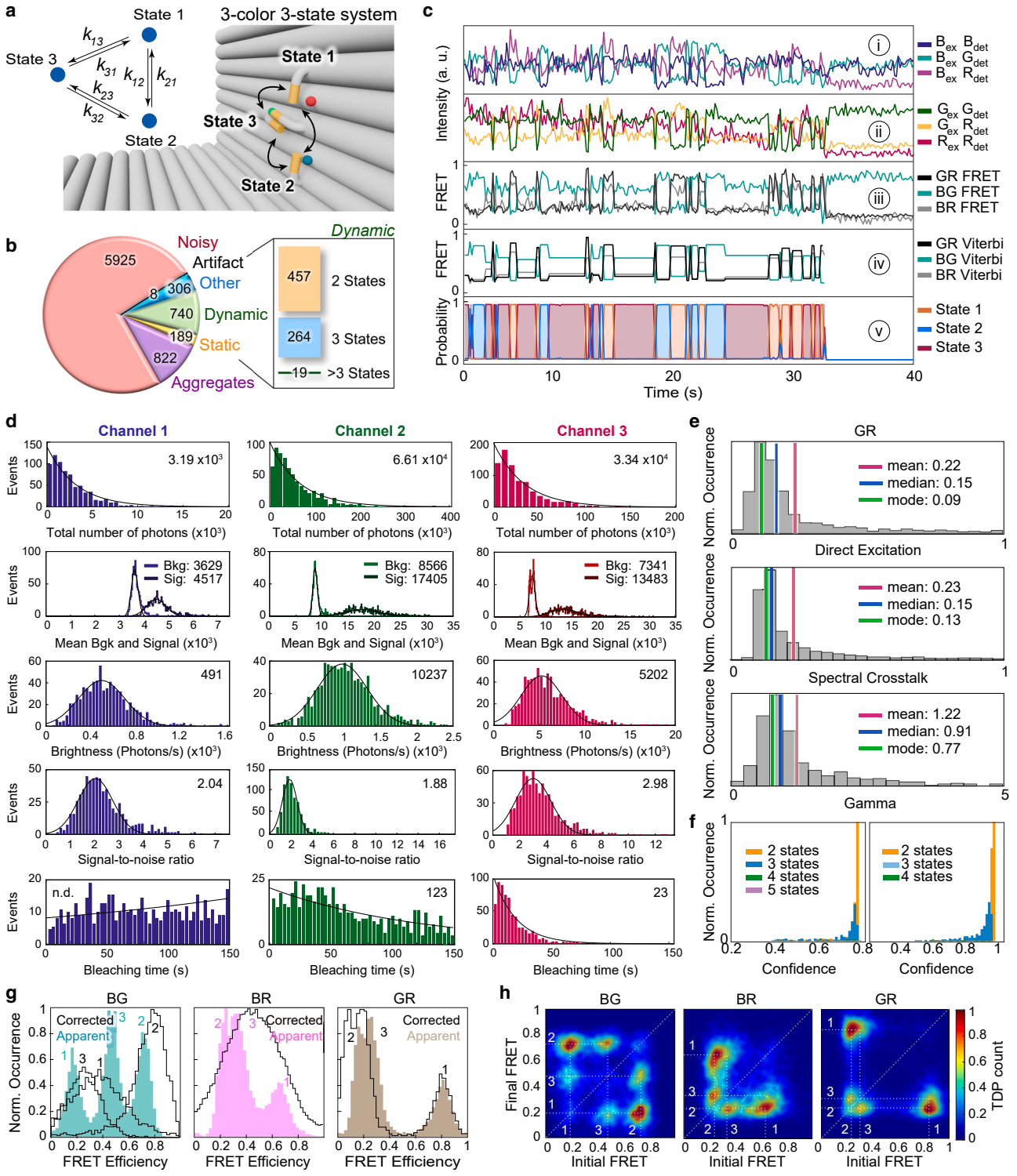

FIGURE 6 Application of the Deep-LASI software for analyzing three-color, three-state smFRET data. (*a*) Schematic overview of an L-shaped DNA origami structure with three binding positions, which are defined as 6, 9 and 12 o'clock. To probe the movement of the tether (labeled with Cy3B), Atto488 and Atto647N are placed near two of the binding sites (6 and 12 o'clock, respectively). The inset shows the corresponding kinetic scheme. (*b*) A pie chart showing the distribution of the 7990 traces that have been sorted into the given categories (Static, Dynamic, Noisy, Aggregate, Artifact, and Other). The 740 dynamic traces have been further categorized based on the number of states observed on each dynamic trace. (*c*) An exemplary single-molecule trace showing the six intensity and three apparent FRET traces for the three-state system. (*i*) The intensity traces detected in the blue, yellow, and red channels after blue excitation. (*ii*) The intensity traces after yellow and red excitation. (*iii*) The corresponding FRET efficiencies for each of the three dye pairs followed by the Viterbi path (*iv*) and state probabilities (*v*) derived by three-color HMM and a deep-learning-assisted kinetic analysis respectively. (*d*)

(legend continued on next page)

as also analyzing partially labeled molecules or performing a series of measurements as a function of experimental conditions that would be otherwise unthinkable when performing a manual analysis.

Compatibility

Although written for the analysis of smFRET data, Deep-LASI is applicable to all single-molecule experiments that end up measuring time traces independent of the setup and raw data file format. The software is compatible with ALEX excitation schemes as well as a non-ALEX excitation for two-color experiments and can read in diverse file formats such as tif, ptu, hdf5, and npz. It is also possible to import other file formats by converting them into a pregiven txt format (13,29). Notably, for measurements with significantly different noise characteristics than those encountered in fluorescence-based methods, the currently incorporated DNNs may need to be retrained.

Adaptability

The development of single-molecule methodologies is a quickly advancing field, and the analysis needs are exceedingly dynamic and often specific for each single project. Accordingly, it should be possible to easily modify and adapt the analysis approaches. Therefore, the source code for Deep-LASI is freely available on the GitLab platform where active feedback and comments can be given (e.g., reporting bugs and suggesting improvements) and users can contribute new functionalities. This is not only possible, but also appreciated.

Unique methods

Deep-LASI combines an easy-to-use manual trace analysis software with state-of-the-art DNNs for automated data processing of one-, two- and three-color data. Many researchers are exploiting the advantages of smFRET but often avoid three-color assays due to the intrinsic complexity of the experiments and time-consuming analysis. Thereby, they also miss out on additional information that can be extracted by adding another fluorophore to the system. In addition, the only other software we are aware of for manually analyzing multicolor smFRET traces is SMACKS (18,39). Unique features of Deep-LASI are the automated analysis of state pathways in kinetic data and its ability to automatically analyze three-color smFRET data and extract absolute distances.

Application of Deep-LASI software on experimental data

Having introduced the Deep-LASI software, we now showcase its application to real three-color experimental data. For this, we show the results from experiments on a previously published L-shaped DNA origami structure (21). The L-shaped origami structure contains a flexible tether that can bind to three distinct states (Fig. 6 *a*). The tether is labeled with Cy3B at the 3′ end and can bind to protruding strands placed at positions referred to as 6, 9 and 12 o'clock. The binding sites consist of complementary ssDNA strands of 7 nt length at 6 and 12 o'clock and 7.5-nt length (i.e. a strand with 8 nt containing a 1 bp mismatch) at 9 o'clock. Binding of the tether occurs by spontaneous base-pairing with the single-stranded protruding strands. To monitor the movement, we introduced two additional fluorophores, Atto488 and Atto647N, on the structure close to the complementary strands at 6 and 12 o'clock positions, respectively.

Data were collected using a three-color ALEX scheme of blue, green and red excitation, and collected on three separate EMCCD cameras. Approximately 8000 traces containing all three fluorophores were extracted from 100 movies. Using the automated neural network analysis, a trace classification was performed. The distribution of classes is shown in Fig. 6 *b*. Of the 7990 traces extracted from the data, a dynamic classification was most probable for 740 (or 9%) of the traces, which were then utilized for further analyses. Fig. 6 *c* shows a representative single-molecule dynamic trace alongside the apparent FRET efficiencies and kinetic analysis. From the selected traces, the software provides an overview of various parameters. Here, we show the total number of photons, the signal and background intensities, the brightness, the signal-to-noise ratio for the BB, GG and RR channels, as well as the time until the photobleaching of the corresponding fluorophore (Fig. 6 *d*). When the measurement is of sufficient quality, one can proceed with the analysis. Next, we analyzed here the regions of the traces selected for determination of the FRET correction factors for spectral crosstalk and direct excitation as well as differences in detection sensitivity (5,6,8) (exemplified in Fig. 4 *e* for the GR dye pair). These are necessary for determining

Photostatistics of the three individual detection channels. The histograms are automatically fit to a Gaussian or exponential functions and the fit parameter reported. Histograms represent the total number of detected photons before photobleaching, the total signal and background (normalized to the number of pixels in the particle mask), the background-corrected molecular brightness, the signal-to-noise ratio and the time until photobleaching of the respective fluorophore. (*e*) Distributions of the FRET correction factors extracted from the data for direct excitation, spectral crosstalk and differences in detection sensitivity (gamma) for the GR FRET pair. The mean, median and mode values for each histogram are indicated in red, blue and green, respectively. (*f*) DNN confidence output for the number of state classifier (*left*) and the state assignment classifier (*right*). (*g*) Apparent frame-wise FRET efficiency histograms are shown as shadowed plots for each dye pair with the three efficiency populations for the BG, BR, and GR pairs. The frame-wise weighted, state-wise corrected FRET histograms are outlined in black. (*h*) TDPs are shown illustrating the transitions detected for all three dye pairs using apparent state-wise FRET efficiencies. (*a*) Is reproduced under the terms of the Creative Common CC-BY 4.0 License (21). Copyright 2023, The Authors. Published by Springer Nature. To see this figure in color, go online.

accurate FRET efficiencies. As neural networks also classify the active fluorophores in each frame, it is possible to extract the maximum number of frames in the data that can be utilized for the individual factors. In addition, for three-color samples, it is also possible to utilize information from the dual-color-labeled complexes. Hence, the automated analysis is often more accurate than the corresponding manually analyzed traces. Traces that exhibit dynamics can then be further analyzed using either HMM or DNNs. Fig. 6 *c*(*iv*–*v*) depicts the Viterbi path of FRET efficiencies and state-probabilities returned from the DNN for the representative smFRET trace. As discussed above, the neural network also generates confidence level histograms (Fig. 6 *e*). The left histogram indicates a large number of traces containing dynamics between two of the states and a significant fraction of traces displaying all three expected states. The right histogram depicts the average confidence of the neural network in assigning the corresponding frames to the two and three states within each trace.

After completing the analysis, the results can be summarized using various tools. For the smFRET data shown here, we compare the frame-wise apparent FRET efficiency histograms (*colored*) and state-wise corrected FRET efficiency histograms (*black lines*) for each dye pair (Fig. 6 *f*). For the BG dye pair, three FRET states are well resolved with apparent efficiency values of 0.18, 0.73, and 0.48, corresponding to states 1, 2, and 3, respectively. As expected from the design and associated Förster radius values of 53 and 65 Å (40–42), the 9 and 12 o'clock positions are more difficult to discern for the BR and GR FRET pairs. Nevertheless, the GR shows three populations with 0.83, 0.22, and 0.30 in apparent FRET efficiency for the same states 1–3. Although applying FRET correction factors in 3cFRET experiments usually results in broadened FRET histograms, the neural network correctly extracts the designed state-wise averaged accurate FRET histograms. Having the additional dimensions available in 3cFRET, it is possible to distinguish the three states. Interestingly, as expected, the three FRET populations in BR converge into a single FRET state at a FRET efficiency of 0.44 upon correction.

Finally, the Deep-LASI software enables the creation of TDPs in separate windows for each dye pair (Fig. 6 *g*). The user can then manually select populations in the plot and fit the resulting dwell-time distributions to determine the underlying transition rates between the corresponding states. By fitting the dwell-time curves (Fig. 6 *h*), we identified state residency times of 0.65, 0.69 and 1.40 s for states 1, 2 and 3, respectively. As the same state trajectories exist for each dye-pair, the state transitions can be selected from the TDPs that provide the best contrast between the two corresponding states.

CONCLUSIONS

In conclusion, Deep-LASI is a software suite that allows for a straightforward and rapid analysis of single-molecule time trajectories. The software supports multiple data formats from a variety of methods such as wide-field and confocal measurements. It allows for the convenient analysis of single-molecule data starting with multiple-channel registration, trace sorting and categorization, determination of the photobleaching steps, calculation of FRET correction factors, and kinetic analyses based on HMM or DNNs. Each step can be performed manually or automatically. It offers advanced functionalities for handling and interpreting single-molecule data in one, two and three colors such as the quantitative analysis of three-color smFRET data. By introducing Deep-LASI, we encourage researchers to exploit the capacities of single-molecule techniques without being concerned about the software environment or complicated, time-consuming analysis steps. As the field develops, the analysis requirements will change. Hence, the software is open source, inviting programming experts to extend the capabilities of Deep-LASI to address the expanding analysis needs of a rapidly growing research field.

DATA AND CODE AVAILABILITY

The software is publicly available as source code, requiring MATLAB or as a precompiled, standalone distribution for Windows or MacOS, and accessible from a GitLab repository at: https://gitlab.com/simon71/deeplasi. A detailed manual can be found at: https://deep-lasi-tutorial.readthedocs.io/en/latest/documentation.html. The experimental data are provided in the Zenodo database (Zenodo: https://zenodo.org/record/7561162).

AUTHOR CONTRIBUTIONS

S.W. developed and implemented the deep learning algorithm, Deep-LASI, in the GUI-based image processing, data extraction and manual analysis software written by C.-B.S. P.A. collected the single-molecule TIRF data. S.W. and P.A. performed the deep-learning-assisted analyses. P.A. wrote the first draft of the manuscript and created the figures. All authors contributed to revising the manuscript. E.P. and D.C.L. supervised the project.

ACKNOWLEDGMENTS

We thank Philipp Messer for valuable input and support regarding implementation of wavelets in the software for particle detection. We thankfully acknowledge the financial support of the Deutsche Forschungsgemeinschaft (DFG, German Research Foundation)—project ID 201269156—SFB 1032 Project B03 (to D.C.L.) and individual grants PL696/4-1 (to E.P.). D.C.L. gratefully acknowledges funding from the Federal Ministry of Education and Research (BMBF) and the Free State of Bavaria under the Excellence Strategy of the Federal Government and the Länder through the ONE MUNICH Project Munich Multiscale Biofabrication. D.C.L. and E.P. gratefully acknowledge the financial support of the Ludwig-Maximilians-Universität München via the Department of Chemistry, the Center for NanoScience (CeNS), and the LMUinnovativ program BioImaging Network (BIN).

DECLARATION OF INTERESTS

The authors declare no competing interests.

REFERENCES

1. Ha, T., T. Enderle, …, S. Weiss. 1996. Probing the interaction between two single molecules: fluorescence resonance energy transfer between a single donor and a single acceptor. *Proc. Natl. Acad. Sci. USA.* 93:6264–6268.
2. Petrosyan, R., A. Narayan, and M. T. Woodside. 2021. Single-Molecule Force Spectroscopy of Protein Folding. *J. Mol. Biol.* 433, 167207.
3. Colson, L., Y. Kwon, …, Y. Cho. 2023. Trends in Single-Molecule Total Internal Reflection Fluorescence Imaging and Their Biological Applications with Lab-on-a-Chip Technology. *Sensors.* 23, 7691.
4. Roy, R., S. Hohng, and T. Ha. 2008. A practical guide to single-molecule FRET. *Nat. Methods.* 5:507–516.
5. Hellenkamp, B., S. Schmid, …, T. Hugel. 2018. Precision and accuracy of single-molecule FRET measurements-a multi-laboratory benchmark study. *Nat. Methods.* 15:669–676.
6. Agam, G., C. Gebhardt, …, T. Cordes. 2023. Reliability and accuracy of single-molecule FRET studies for characterization of structural dynamics and distances in proteins. *Nat. Methods.* 20:523–535.
7. Ha, T., A. Y. Ting, …, S. Weiss. 1999. Single-molecule fluorescence spectroscopy of enzyme conformational dynamics and cleavage mechanism. *Proc. Natl. Acad. Sci. USA.* 96:893–898.
8. Lerner, E., A. Barth, …, S. Weiss. 2021. FRET-based dynamic structural biology: Challenges, perspectives and an appeal for open-science practices. *Elife.* 10, e60416.
9. Kapanidis, A. N., N. K. Lee, …, S. Weiss. 2004. Fluorescence-aided molecule sorting: Analysis of structure and interactions by alternating-laser excitation of single molecules. *Proc. Natl. Acad. Sci. USA.* 101:8936–8941.
10. Hildebrandt, L. L., S. Preus, and V. Birkedal. 2015. Quantitative single molecule FRET efficiencies using TIRF microscopy. *Faraday Discuss.* 184:131–142.
11. Salem, C.-B., E. Ploetz, and D. C. Lamb. 2019. Probing dynamics in single molecules. *In* Spectroscopy and Dynamics of Single Molecules, pp. 71–115.
12. Kudryavtsev, V., M. Sikor, …, D. C. Lamb. 2012. Combining MFD and PIE for accurate single-pair Forster resonance energy transfer measurements. *ChemPhysChem.* 13:1060–1078.
13. Götz, M., A. Barth, …, S. Schmid. 2022. A blind benchmark of analysis tools to infer kinetic rate constants from single-molecule FRET trajectories. *Nat. Commun.* 13:5402.
14. de Lannoy, C. V., M. Filius, …, D. de Ridder. 2021. FRETboard: Semi-supervised classification of FRET traces. *Biophys. J.* 120:3253–3260.
15. Huisjes, N. M., T. M. Retzer, …, K. E. Duderstadt. 2022. Mars, a molecule archive suite for reproducible analysis and reporting of single-molecule properties from bioimages. *Elife.* 11, e75899.
16. Kinz-Thompson, C. D., and R. L. Gonzalez, Jr. 2018. Increasing the Time Resolution of Single-Molecule Experiments with Bayesian Inference. *Biophys. J.* 114:289–300.
17. Preus, S., S. L. Noer, …, V. Birkedal. 2015. iSMS: single-molecule FRET microscopy software. *Nat. Methods.* 12:593–594.
18. Schmid, S., M. Götz, and T. Hugel. 2016. Single-Molecule Analysis beyond Dwell Times: Demonstration and Assessment in and out of Equilibrium. *Biophys. J.* 111:1375–1384.
19. Verma, A. R., K. K. Ray, …, R. L. Gonzalez. 2023. Increasing the accuracy of single-molecule data analysis using tMAVEN. Preprint at bioRxiv. https://doi.org/10.1101/2023.08.15.553409.
20. Heiss, G., E. Ploetz, …, D. C. Lamb. 2019. Conformational changes and catalytic inefficiency associated with Mot1-mediated TBP–DNA dissociation. *Nucleic Acids Res.* 47:2793–2806.
21. Wanninger, S., P. Asadiatouei, …, D. C. Lamb. 2023. Deep-LASI: deep-learning assisted, single-molecule imaging analysis of multi-color DNA origami structures. *Nat. Commun.* 14:6564.
22. Thomsen, J., M. B. Sletfjerding, …, N. S. Hatzakis. 2020. DeepFRET, a software for rapid and automated single-molecule FRET data classification using deep learning. *Elife.* 9:e60404.
23. Li, J., L. Zhang, …, N. G. Walter. 2020. Automatic classification and segmentation of single-molecule fluorescence time traces with deep learning. *Nat. Commun.* 11:5833.
24. Liao, J., J. Qu, …, J. Li. 2022. Deep-learning-based methods for super-resolution fluorescence microscopy. *J. Innov. Opt. Health Sci.* 16 (03)
25. Yao, R., M. Ochoa, …, X. Intes. 2019. Net-FLICS: fast quantitative wide-field fluorescence lifetime imaging with compressed sensing - a deep learning approach. *Light Sci. Appl.* 8:26.
26. Huang, B., J. Li, …, J. Qu. 2023. Enhancing image resolution of confocal fluorescence microscopy with deep learning. *PhotoniX.* 4, 2.
27. Ragone, M., R. Shahabazian-Yassar, …, V. Yurkiv. 2023. Deep learning modeling in microscopy imaging: A review of materials science applications. *Prog. Mater. Sci.* 138, 101165.
28. Fablab. 2023. Deep-LASI Documentation. https://deep-lasi-tutorial.readthedocs.io/en/latest/index.html.
29. Deep-LASI. 2023. Deep-LASI Software. https://gitlab.com/simon71/deeplasi.
30. Reddy, B. S., and B. N. Chatterji. 1996. An FFT-based technique for translation, rotation, and scale-invariant image registration. *IEEE Trans. Image Process.* 5:1266–1271.
31. Mallat, S. G. 1989. A theory for multiresolution signal decomposition: the wavelet representation. *IEEE Trans. Pattern Anal. Mach. Intell.* 11:674–693.
32. Kapanidis, A. N., T. A. Laurence, …, S. Weiss. 2005. Alternating Laser Excitation of Single Molecules. *Acc. Chem. Res.* 38:523–533.
33. Daubechies, I. 1992. Ten Lectures on Wavelets. SIAM.
34. Mallat, S. G. 2009. A Wavelet Tour of Signal Processing : The Sparse Way, 3rd ed. Elsevier/Academic Press, p. 805.
35. Starck, J. L., and F. Murtagh. 2007. Astronomical Image and Data Analysis. Springer Berlin Heidelberg.
36. Schreiber, J. 2018. Pomegranate: fast and flexible probabilistic modeling in python. *J. Mach. Learn. Res.* 18:1–6.
37. Murphy, K. 1998. Hidden markov model (HMM) toolbox for Matlab. http://www.cs.ubc.ca/∼murphyk/Software/HMM/hmm.html.
38. Barth, A., L. Voith von Voithenberg, and D. C. Lamb. 2019. Quantitative Single-Molecule Three-Color Forster Resonance Energy Transfer by Photon Distribution Analysis. *J. Phys. Chem. B.* 123:6901–6916.
39. Götz, M., P. Wortmann, …, T. Hugel. 2016. A Multicolor Single-Molecule FRET Approach to Study Protein Dynamics and Interactions Simultaneously. *Methods Enzymol.* 581:487–516.
40. Ploetz, E., E. Lerner, …, T. Cordes. 2016. Förster resonance energy transfer and protein-induced fluorescence enhancement as synergetic multi-scale molecular rulers. *Sci. Rep.* 6, 33257.
41. Atto-Tec. 2023. Förster Radius of Atto dyes. https://www.atto-tec.com/images/ATTO/Katalog_Preisliste/Katalog_2019_2020.pdf.
42. Ross, J., P. Buschkamp, …, P. Tinnefeld. 2007. Multicolor Single-Molecule Spectroscopy with Alternating Laser Excitation for the Investigation of Interactions and Dynamics. *J. Phys. Chem. B.* 111:321–326.